IEEE Access
Multidisciplinary | Rapid Review | Open Access Journal

Received 5 January 2024, accepted 27 January 2024, date of publication 30 January 2024, date of current version 8 February 2024.

Digital Object Identifier 10.1109/ACCESS.2024.3360133

RESEARCH ARTICLE

Improving Connectivity in 6G Maritime Communication Networks With UAV Swarms

NIKOLAOS NOMIKOS[1], (Senior Member, IEEE), ANASTASIOS GIANNOPOULOS[1], (Member, IEEE), ALEXANDROS KALAFATELIS[1], (Graduate Student Member, IEEE), VOLKAN ÖZDURAN[2], (Member, IEEE), PANAGIOTIS TRAKADAS[1], AND GEORGE K. KARAGIANNIDIS[3,4], (Fellow, IEEE)

[1]Department of Ports Management and Shipping, National and Kapodistrian University of Athens, 34400 Euboea, Greece
[2]Istanbul University-Cerrahpaşa, Istanbul 34320, Turkey
[3]Department of Electrical and Computer Engineering, Aristotle University of Thessaloniki, 546 36 Thessaloniki, Greece
[4]Cyber Security Systems and Applied AI Research Center, Lebanese American University (LAU), Beirut, Lebanon

Corresponding author: Nikolaos Nomikos (nomikosn@pms.uoa.gr)

This work was supported in part by the HORSE project, funded by the Smart Networks and Services Joint Undertaking (SNS JU) through the European Union's Horizon Europe Research and Innovation Programme under Grant 101096342 (www.horse-6g.eu).

ABSTRACT The deployment of maritime communication networks (MCNs) enables Internet-of-Things (IoT) applications, related to autonomous navigation, offshore facilities and smart ports. Still, the majority of maritime nodes, residing in MCNs lacks reliable connectivity. Towards this end, integrating unmanned aerial vehicles (UAVs) in sixth generation (6G) MCN topologies results in the formation of an aerial segment, complementing shore base stations that may offer insufficient coverage, and satellite communication, characterized by increased delays. In this study, we focus on an MCN where the direct links towards a shore BS are not available, due to excessive fading conditions. For this case, we use a UAV swarm to provide improved wireless connectivity, adopting non-orthogonal multiple access (NOMA) for high resource efficiency. In downlink communication, UAVs take into consideration the desired service rate and the channel quality of their links towards the maritime nodes. In the uplink, UAVs employ dynamic decoding ordering to enhance the performance of successive interference cancellation, avoiding fixed ordering of the maritime nodes' signals. Moreover, to ensure highly flexible UAV selection, UAVs are equipped with buffers to store data. Performance comparisons show that the UAV swarm-aided MCN enjoys increased average sum-rate by relying on multi-criteria-based interference cancellation and buffer-aided UAVs, over other benchmark schemes in the downlink and uplink. Finally, the delay-aware nature of the proposed algorithms where the UAV-destination links are prioritized, leads to reduced average delay.

INDEX TERMS 6G, buffer-aided, maritime communication network (MCN), maritime IoT, NOMA, swarms, UAV.

I. INTRODUCTION

Fifth generation (5G) mobile networks provide services to coexisting Internet-of-Things (IoT) nodes and mobile users that are usually deployed in urban settings [1], [2], [3]. As a consequence, the majority of network deployments and wireless technologies has been supported by land-based topologies, while important innovations have not been integrated in maritime communication networks (MCNs). Currently, MCNs mainly rely on satellites, characterized by increased latency and limited data rates [4]. Considering that important economic activities are based on maritime

The associate editor coordinating the review of this manuscript and approving it for publication was Stefano Scanzio.

transportation, and a broad range of maritime applications, such as ocean monitoring, and offshore facilities operation must be reliably and efficiently supported, a paradigm shift in MCNs is required [5]. Thus, the recent introduction unmanned aerial vehicles (UAVs) into wireless networks constitutes a major enabler to provide ubiquitous coverage and connectivity at sea [6], [7], [8], [9]. In greater detail, UAVs offer in a dynamic fashion, wireless resources to improve the Quality-of-Service (QoS), while allowing autonomous operation, ensuring maximum reliability through increased diversity and ultra low-latency by providing broadband connectivity at the network edge.

Considering these advantages, it is vital to examine the potential of UAVs to support MCNs, exploiting sixth generation (6G) communication technologies. In this work, an MCN is studied where a swarm of UAVs is deployed to establish connectivity of heterogeneous maritime nodes with a shore base station (BS) in both downlink and uplink directions. Moreover, for increased wireless resource efficiency, the maritime nodes are concurrently served through non-orthogonal multiple access (NOMA). In this case, in the downlink, UAVs employ superposition coding and determine power allocation, according to the desired service rate and channel state information (CSI). In addition, in the uplink, each member of the swarm successively decodes the received data prior to relaying the decoded packets to the shore BS. In this case, UAVs employ dynamic decoding ordering to enhance the performance of successive interference cancellation (SIC), using only CSI at the reception.

A. MARITIME COMMUNICATION NETWORKS

MCNs enable a wide gamut of IoT services, such as navigation of autonomous vehicles, connectivity and monitoring of offshore facilities, ocean exploration, environmental data collection, and real-time video transmission during search and rescue (SAR) operations [10]. MCNs consist of different vessels, platforms, buoys, unmanned surface/underwater vehicles (USVs/UUVs), sensors, and actuators [7]. Moreover, applications in the maritime domain require varying QoS levels. Mobile users at cruise ships desire ubiquitous and broadband connectivity while for SAR operations, it is necessary to transmit high definition multimedia content. Finally, ultra-reliable and ultra-low latency communication (URLLC) is necessary for maritime IoT applications and intelligent transportation systems [11], [12].

At the moment, wireless connectivity for MCNs is usually provided by shore BSs and satellite systems. Unfortunately, these topologies have important shortcomings, including insufficient data rates and excessive communication delays, mainly by the satellite segment, as well as limited spectrum availability, and intermittent connectivity. In recent years, industrial actors have aimed at improving the quality of coverage provided by satellites and shore BSs [13], [14]. However, the potential of UAVs to mitigate path-loss, reduce latency and improve communication reliability has not been unlocked. In this context, developing flexible algorithms for UAV-aided resource provisioning in MCNs is essential.

B. UAV-AIDED WIRELESS NETWORKS

The road to realize 6G networking includes radical departures from conventional wireless architectures, where highly dynamic nodes are deployed to different network areas, ensuring increased resiliency against outages [15], [16]. Moreover, UAVs act as an intermediate layer to terrestrial and satellite segments, providing connectivity in remote and rural environments, fast recovery from disasters, and on-demand radio-resources [7], [17], [18], [19]. In [7], the authors have studied the role of deployable BSs, both UAVs and mobile vessels, for maritime coverage enhancement, resulting in a hierarchical satellite-UAV-terrestrial network. In this setting, they develop a joint link scheduling and rate adaptation scheme, exploiting only location-dependent large-scale CSI to minimize the total energy consumption with QoS guarantees. In MCNs, the UAVs' ability to support terrestrial and satellite networks for providing broadband and URLLC services to various maritime activities, supporting SAR operations and surface/underwater IoT services has attracted significant interest [20], [21]. For these applications, UAVs can assume the role of wireless relays, providing long-range communication through multi-hop communication. In underwater deployments, UAVs facilitate data collection and edge processing by working in tandem with USVs and UUVs [22]. In addition, in SAR operations, UAVs are able to establish line-of-sight (LoS) and high-capacity connectivity for high definition video streaming to shore BSs and human operators in control centers.

Focusing on the use of NOMA in UAV-aided MCNs, a small number of works has provided relevant algorithms and performance evaluation results. In [23], a collaborative network is deployed, located close to the shore, relying on UAVs and a shore BS to form user-centric clusters. In each cluster, sparsely distributed maritime IoT devices are concurrently supported through NOMA while the nearshore network shares its spectral resource with satellites. In this topology, power allocation for sum-rate maximization and interference mitigation between network layers, clusters, and users are conducted. Furthermore, the authors employ iterative power allocation to ensure improved wireless access, over other NOMA and orthogonal multiple access (OMA) approaches. However, this work considers the existence of a satellite network without standalone UAV swarm communication with the shore network. Then, the study in [24] examines NOMA groups, consisting of vessels that are connected with UAVs or shore BSs. Towards reducing system cost, a UAV with a single antenna and optimized trajectory has been deployed, exploiting vessel location in blind zones. This non-convex problem is decomposed

into two subproblems, i.e. transmit power allocation and time allocation. Simulation results reveal improved spectral efficiency, compared to an equivalent MCN, relying on OMA. Still, this work only considers the downlink communication and does not provide a holistic downlink/uplink perspective on the MCN operation. Focusing on energy efficiency, the works in [25] and [26] use UAVs to gather data from surface sink nodes (SNs) which are responsible for controlling underwater sensor nodes (USNs) and forward this data to a shore BS. Aiming at MCN lifetime maximization, optimized resource allocation and UAV deployment are considered. This joint problem is then decoupled into a UAV-SN delay minimization and a USN-SN lifetime maximization subproblem. Performance results highlight increased energy efficiency and longer network lifetime, compared to OMA-based schemes. Nonetheless, MCN operation and related issues in the downlink are not explored.

In this work, we use a UAV swarm to improve connectivity in 6G MCNs. Towards this end, we extend the UAV-aided framework for MCNs, presented in [27], by modelling and evaluating both downlink and uplink communication scenarios, in terms of average sum-rate and delay. In addition, we discuss implementation issues related to centralized and distributed operation for the proposed algorithms and obtain their complexity order with regard to coordination and signalling overheads. Specifically, an MCN topology is investigated where direct communication from/to a shore BS is not possible, as a result of severe fading conditions. Thus, a swarm of UAVs is introduced, acting as wireless relays, simultaneously serving multiple maritime nodes, and supporting services with varying QoS requirements. Furthermore, as UAVs have buffering capabilities for storing data, highly flexible opportunistic UAV selection is performed, significantly improving the MCN's reliability.

C. CONTRIBUTIONS

As it is evident from the previous discussion on relevant works, several aspects of UAV swarm-aided MCNs have not been thoroughly studied. Such aspects include flexible UAV selection policies, centralized and distributed implementation, and the simultaneous integration of NOMA anddata buffering at the UAVs. Thus, in this work, we provide the following contributions:

- In the considered MCN downlink, a member of the UAV swarm is activated to serve as a relay, concurrently transmitting towards the maritime nodes using NOMA. In this scheme, the activated UAV adopts NOMA where power allocation considers both the desired rate and the CSI of the maritime nodes. Meanwhile, another UAV is selected to receive new packets from the shore BS, achieving full-duplex (FD) operation through successive relaying. For the proposed algorithm, implementation and complexity issues are thoroughly discussed.
- In the MCN uplink, we depart from the scheme of [25] and [26], by prompting UAVs to perform dynamic decoding ordering and increase the probability for successful SIC without requiring full CSI to be acquired by the maritime nodes that may have limited energy and processing capabilities. Again, centralized and distributed implementation details and the complexity order are provided.
- For both schemes, an MCN topology with multiple maritime nodes is simulated and average sum-rate and latency results reveal that in downlink communication scenarios, the UAV swarm-aided and multi-criteria NOMA-based MCN provides increased communication reliability over OMA alternatives. Furthermore, in the uplink, our UAV swarm-aided NOMA scheme leverages the low-complexity dynamic decoding ordering and achieves higher sum-rate over OMA alternatives. More importantly, despite the use of buffers at the UAVs that increase MCN reliability, the delay-aware nature of the proposed algorithms, prioritizing the UAV-destination links, leads to reduced average delay and improved sum rate-delay trade-off over other multiple access solutions.

TABLE 1. List of acronyms.

5G	Fifth generation
6G	Sixth generation
ACK	Acknowledgement
AWGN	Additive white Gaussian noise
BA	Buffer-aided
BS	Base station
BSI	Buffer state information
BUN	Buffer-aided and UAV-based NOMA
CSI	Channel state information
CSIT	CSI at the transmitter
DF	Decode-and-forward
DoF	Degrees of freedom
HD	Half-duplex
IoT	Internet-of-Things
IRI	Inter-relay interference
LoS	Line-of-sight
MCN	Maritime communication network
NACK	Negative ACK
NFV	Network function virtualization
NLoS	Non-LoS
NOMA	Non-orthogonal multiple access
O-RAN	Open radio access network
OMA	Orthogonal multiple access
QoS	Quality-of-Service
SAR	Search and rescue
SIC	Successive interference cancellation
SINR	Signal-to-interference-plus-noise ratio
SN	Sink node
SNR	Signal-to-noise ratio
TDMA	Time-division multiple access
UAV	Unmanned aerial vehicle
URLLC	Ultra-reliable and ultra-low latency
USN	Underwater sensor node
USV	Unmanned surface vehicle
UUV	Unmanned underwater vehicle

D. STRUCTURE

In what follows, Section II presents the system model, as well as the necessary preliminaries for this study. Next, Section III offers details on the downlink UAV swarm-aided and

TABLE 2. Summary of notation.

α_k	Power allocation coefficient
γ_{ij}	Capture ratio for successfully receiving the signal over the $\{i \rightarrow j\}$ link
Γ_{ij}	SNR in the $\{i \rightarrow j\}$ link
σ_l^2	Variance of the thermal noise at the l-th receiver
σ_{ij}^2	Variance of the $\{i \rightarrow j\}$ link's fading coefficient
ϕ_k	Signal ordering permutation at the k-th UAV
Φ	Set of all possible decoding orders
b_{ij}	Set of binary elements containing links that do not experience an outage
c	Speed of light
$\mathcal{C}$	Set of UAV relays
d_{ij}	Distance between node i and node j
D	Destination
f	Carrier frequency
$\mathcal{F}_{ij}$	Set of feasible $\{i \rightarrow j\}$ links
g_{ij}	Channel gain of link $\{i \rightarrow j\}$
h_{ij}	Channel coefficient, comprising both small- and large-scale fading effects
h_U	Altitude of the UAV
K	Number of UAV relays
L	Buffer size (in packets)
L_{ij}	Large-scale fading coefficient
L_n	Size of the n-th sub-buffer
N	Number of maritime sources
P_n	Power level of the n-th source
q_{ij}	Set of binary elements containing links that fulfill the buffer conditions
Q_k	k-th buffer
$Q_{k,n}$	n-th sub-buffer of the k-th buffer
r_i	Data rate of the i-th transmitter
R_k	k-th relay nod
s_{ij}	Small-scale fading coefficient of the $\{i \rightarrow j\}$ link
S_n	n-th source

NOMA-based MCN. Section IV provides in detail, the uplink dynamic decoding ordering strategy for the UAV swarm-aided MCN. Then, average sum-rate and delay performance comparisons are given and discussed in Section V. Finally, Section VI provides the conclusions of our study and a number of future research directions, aiming to stimulate further interest in UAV swarm-aided MCNs.

Table 1 includes the list of acronyms, while Table 2 provides the notation used throughout the paper.

II. SYSTEM MODEL

A. NETWORK MODEL

A UAV swarm-aided MCN is considered, comprising a single shore BS, N maritime nodes, such as USVs, buoys and offshore platforms and a swarm $\mathcal{C}$ of K decode-and-forward (DF) half-duplex (HD) relays UAVs, having the role of wireless relay nodes, $R_k \in \mathcal{C}$ $(1 \leq k \leq K)$. The UAV swarm-aided MCN is depicted in Fig. 1. In the downlink, the shore BS acts as the information source, S, having packets to transmit towards the N maritime nodes, denoted as D_n $(1 \leq n \leq N)$. In the uplink, the maritime nodes are the information sources, denoted as S_n $(1 \leq n \leq N)$ and the shore BS is the intended destination, D, receiving the packets from the N maritime nodes. Due to increased fading, direct

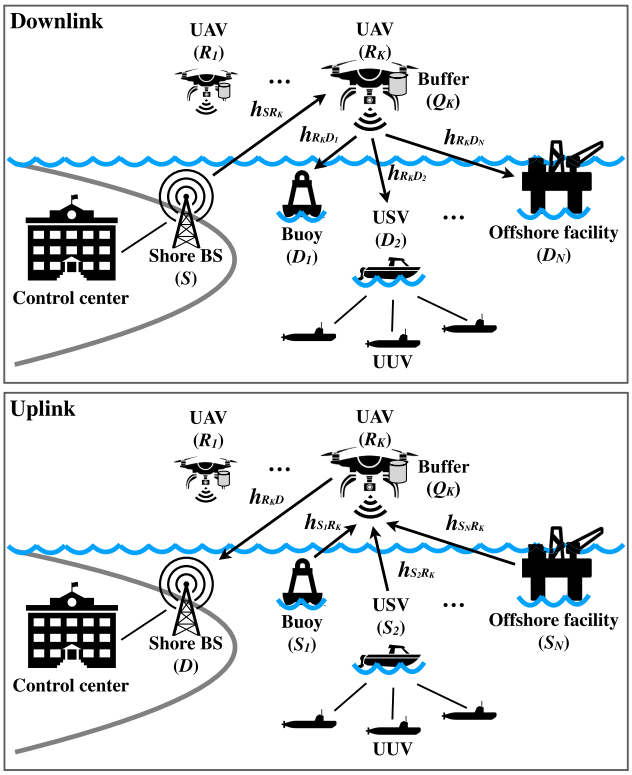

FIGURE 1. A UAV swarm-aided MCN in the downlink and uplink.

communication among the shore BS and the maritime nodes is not possible and wireless connectivity can only be provided by the UAVs. Each UAV has two buffers, each with size L, in packets. In each communication direction, we denote the amount of stored packets in UAV R_k's buffer by Q_k and its capacity is equally allocated among the maritime nodes i.e., the same amount of packets can be stored at each UAV. Thus, sub-buffers, denoted as $Q_{k,n}$ are formed and their sub-buffer sizes, being equal for all UAVs are denoted by L_n.

The information sources, i.e. a shore BS in the downlink or N maritime nodes in the uplink are saturated and always have packets from transmission and the required data rate, r_{BS}, r_{S_n} is fixed and might be different, depending on the desired maritime application. As an example, if S_1 is a USV, responsible for multiple UUVs, patrolling maritime infrastructures and S_2 is a buoy, conducting environmental monitoring, their rate requirements will not be the same and, hence, $r_{S_1} \neq r_{S_2}$. Similarly, a transmission from node i towards node j will be feasible, as long as the signal-to-noise ratio (SNR) Γ_{ij} is above the capture ratio γ_{ij}. In greater detail, γ_{ij} is defined as $\gamma_{ij} = 2^{r_i - 1}$, where r_i stems from the maritime application's modulation and coding parameters. In addition, at an arbitrary time-slot, the shore BS, the UAVs or the maritime nodes aim at transmitting their data, with a power level P_i, $i \in \{S, S_1, \ldots, S_N, R_1, \ldots, R_K\}$.

It should be noted that acknowledgement/negative-acknowledgement (ACKs/NACKs) are used for packet retransmissions, broadcasted by the receivers. As multiple

UAVs might receive the same packets, the MCN should have the ability to notify them which packet ID(s) has been successfully received by the destination. Thus, we consider that ACKs include the packet ID, facilitating UAVs to discard redundant information and avoid transmitting duplicate packets at a future time-slot.

B. CHANNEL MODEL

In the considered UAV swarm-aided topology, each wireless link experiences additive white Gaussian noise (AWGN), frequency non-selective small-scale block fading, following a zero mean complex Gaussian distribution with variance σ_{ij}^2, and large-scale path-loss fading. Also, it is characterized by a complex channel coefficient s_{ij}, and the channel gain, $g_{ij} \triangleq |s_{ij}|^2$, is exponentially non-identically distributed i.e., $g_{ij} \sim \text{Exp}(\lambda_{ij})$, $\lambda_{ij} > 0$. Moreover, The thermal noise at a receiver l is characterized by zero mean and variance denoted by σ_l^2, $l \in \{R_1, R_2, \ldots, R_K, D, D_1, \ldots, D_N\}$, being AWGN distributed.

The maritime channel has both LoS and non-LoS (NLoS) components, and the probability of LoS is determined by the elevation angle among the shore BS/maritime node and the members of the UAV swarm, as well as the scatterers density and height in the coverage area [28] while the coefficient of large-scale fading is given below as [24] and [29]

$$L_{ij}^{\text{dB}} = \frac{\eta_{LoS} - \eta_{NLoS}}{1 + \alpha e^{-b(\rho_{ij} - \alpha)}} + B_{ij}; \tag{1}$$

where

$$B_{ij} = 20\log_{10}(d_{ij}) + 20\log_{10}(\frac{4\pi f}{c}) + \eta_{NLoS}; \tag{2}$$

$$\rho_{ij} = \frac{180}{\pi}\arcsin(\frac{h_U}{d_{ij}}); \tag{3}$$

where the carrier frequency is denoted by f, the speed of light by c, while η_{LoS}, η_{NLoS}, α, b correspond to propagation environment constants, d_{ij} is the distance between node i and node j, and h_U denotes the altitude of the UAV.

Thus, large-scale channel fading is given as

$$L_{ij} = 10^{-\frac{L_{ij}^{\text{dB}}}{10}}. \tag{4}$$

Therefore, the channel coefficient, comprising the effects of small-scale and large-scale fading is calculated as

$$h_{ij} = L_{ij}^{1/2} s_{ij}. \tag{5}$$

III. DOWNLINK

In this section, details for the case of downlink communication where the shore BS transmit towards the N maritime nodes through the K UAVs are provided.

A. {S→R} LINK TRANSMISSION

In the considered MCN, each time-slot is allocated to successive transmissions in both hops by the shore BS and a member of the UAV swarm, in order to achieve FD downlink operation. Thus, when a UAV R_k is selected for transmission, the remaining $K-1$ UAVs will experience inter-relay interference (IRI) while receiving the packet of the shore BS. Regarding the shore BS broadcast transmission, without loss of generality, a case involving two maritime nodes, being simultaneously served in each time-slot is considered. Here, each maritime node might desire a different service rate r_j, $j \in \{1, 2\}$, and the shore BS transmits with rate $r_1 + r_2$ [30] to avoid buffer overflow or underflow. Thus, link SR_i, $i \neq k$ will not experience an outage when

$$\Gamma_{SR_i}(P_S) \triangleq \frac{g_{SR_i} L_{SR_i} P_S}{g_{R_k R_i} L_{R_k R_i} P_{R_k} + \sigma_i^2} \geq 2^{r_1+r_2} - 1. \tag{6}$$

On the other hand, link SR_i will be in outage if $\gamma_{R_i} < 2^{r_1+r_2} - 1$, and this probability is expressed as

$$p_{\text{out}\{S\to R\}} \triangleq \mathbb{P}\left[g_{SR_i} < \frac{(2^{r_1+r_2} - 1)(g_{R_k R_i} L_{R_k R_i} P_{R_k} + \sigma_i^2)}{P_S} \right]. \tag{7}$$

The vector $b_{SR} \triangleq \left(b_{SR_1}, b_{SR_2}, \ldots, b_{SR_K}\right)$ consisting of binary elements contains the $\{S\to R\}$ links that do not experience an outage. This, in case the transmission on link SR_i can be performed, then $b_{SR_i} = 1$. Correspondingly, binary elements $q_{SR} \triangleq \left(q_{SR_1}, q_{SR_2}, \ldots, q_{SR_K}\right)$ represent the feasible $\{S\to R\}$ links, fulfilling the buffer conditions. More specifically, these conditions are satisfied when buffers have available space to support the $\{S\to R\}$ transmissions. Set $\mathcal{F}_{SR}$ contains the feasible $\{S\to R\}$ links. If $b_{SR_i} = 0$ or $q_{SR_i} = 0$, the source signal on link SR_i cannot be transmitted and thus, this link is considered to be in outage.

B. {R→D} LINK TRANSMISSION

When UAV R_k is activated to transmit, the information signal for the two maritime destinations D_1 and D_2 are superimposed, according to NOMA. The transmitted signal, comprising the information signals x_1 and x_2 of the maritime nodes, is given as

$$x = \sqrt{\alpha_k} x_1 + \sqrt{1 - \alpha_k} x_2, \tag{8}$$

with $\mathbb{E}[|x_1|^2] = \mathbb{E}[|x_2|^2] = 1$ and $0 \leq \alpha_k \leq 1$, where α_k is the power allocation coefficient.

Then, D_1 receives signal y_1, containing the desired symbol, as well as the symbol for D_2, i.e.,

$$y_1 = s_{R_k D_1}\sqrt{\alpha_k P_{R_k}} x_1 + s_{R_k D_1}\sqrt{(1-\alpha_k) P_{R_k}} x_2 + \eta_1, \tag{9}$$

correspondingly, the received signal y_2 at D_2 is described as

$$y_2 = s_{R_k D_2}\sqrt{\alpha_k P_{R_k}} x_1 + s_{R_k D_2}\sqrt{(1-\alpha_k) P_{R_k}} x_2 + \eta_2, \tag{10}$$

where the AWGN at each maritime node is denoted as η_1 and η_2.

As in this MCN, NOMA in the power-domain is adopted, the transmitting UAV R_k should properly set the power allocation coefficients α_k for the superimposed signals.

Considering that the UAVs have full availability of the $\{R\rightarrow D\}$ CSI, power allocation is performed at each time-slot. In this case, α_k is set accordingly to enhance SIC performance, considering that the received signal-to-interference-plus-noise ratio (SINR) must be above the capture ratio at both maritime nodes. This process is adopted by all the UAVs in the swarm, resulting in the formation of the set of candidate UAVs, being able to allow NOMA operation in the $\{R\rightarrow D\}$ links.

For example, x_2's decoding at D_1 and D_2 is performed as

$$\Gamma_{R_kD_j}(P_{R_k}) = \frac{(1-\alpha_k)P_{R_k}g_{R_kD_j}L_{R_kD_j}}{\alpha_k P_{R_k}g_{R_kD_j}L_{R_kD_j}+\sigma^2_{D_j}} \geq \gamma_j, \quad j\in\{1,2\}. \tag{11}$$

Note that $\gamma_j \equiv 2^{r_j}-1$. As soon as x_2 has been decoded and subtracted, x_1 is decoded at D_1, without interference

$$\Gamma_{R_kD_1}(P_{R_k}) = \frac{\alpha_k P_{R_k}g_{R_kD_1}L_{R_kD_1}}{\sigma^2_{D_1}} \geq \gamma_1. \tag{12}$$

Here, the power allocation method in [31] is employed, being developed for multi-relay deployments, comprising destinations with different service rate requirements, and readers are referred to that study, providing the detailed steps for calculating α_k.

The $\{R\rightarrow D\}$ link outage probability in the case of NOMA is equal to

$$p_{\text{out}\{R\rightarrow D\}} = \mathbb{P}\left[\alpha_{k,\min} > \min\{1,\alpha_{k,\max}\}\right]. \tag{13}$$

where $\alpha_{k,\min}$ and $\alpha_{k,\max}$ have been given in [31].

Let vector $b_{RD} \triangleq \left(b_{R_1D}, b_{R_2D}, \ldots, b_{R_KD}\right)$ denote the binary representation of the $\{R\rightarrow D\}$ links fulfilling eqs. (11), (12) and thus, if NOMA can be performed on the set of links $\{R_k \rightarrow D_1\}$, $\{R_k \rightarrow D_2\}$, then $b_{R_kD} = 1$. Likewise, the binary representation of feasible links are included in vector $q_{RD} \triangleq \left(q_{R_1D}, q_{R_2D}, \ldots, q_{R_KD}\right)$, i.e. links with a UAV that satisfy the buffer conditions by having stored data. By $\mathcal{F}_{RD}$ we denote the set of feasible $\{R\rightarrow D\}$ links with cardinality F_{RD}.

C. BUN-DL ALGORITHMIC DESCRIPTION

The proposed buffer-aided (BA) and UAV-based NOMA in the downlink (BUN-DL) aims at increasing the sum-rate of MCNs without necessitating the availability of multiple antennas at the UAVs or the availability of CSI at the shore BS. BUN-DL integrates successive shore BS and UAV transmissions at the expense of IRI, leveraging buffering at the UAVs for increased scheduling flexibility and NOMA to improve spectral efficiency.

In each time-slot, each UAV R_k, follows the steps described in Algorithm 1. First, BUN-DL selects a UAV R_k to serve D_1 and D_2 using NOMA. The selection is based on the availability of $\{R\rightarrow D\}$ CSI of the maritime nodes to decide if NOMA can be performed, and the UAVs' buffer state information (BSI) to find which one has the largest buffer length (line 1). Then, candidate UAV R_k derives the coefficient of power allocation, based on the corresponding $\{R\rightarrow D\}$ CSI (line 2). At the same time, following a distributed method, R_k's timer is set inversely proportional to the amount of stored packets Q_k (lines 3, 4). When the transmitting UAV is activated (line 5), $\{S\rightarrow R\}$ broadcasting and $\{R\rightarrow D\}$ transmission are concurrently employed, and the other $K-1$ UAVs attempt the reception of the shore BS's signal, containing the signals intended for D_1 and D_2 at a rate $r = r_1 + r_2$, while experiencing IRI by the transmitting UAV (lines 6, 7). The use of broadcasting in the MCN allows a higher number of packets to be available at the UAVs' buffers and does not require CSI to be available at the shore BS, thus minimizing the implementation complexity. In case a transmitting UAV was not selected, all K UAVs listen to the shoe BS's broadcast transmission, as long as their buffers are not full (line 10). Finally, when the two maritime nodes D_1 and D_2 receive packets from the transmitting UAV, they will transmit ACKs with the packets IDs to all the UAVs in swarm, triggering them to drop the corresponding packets from their queues (line 12). It must be noted that BUN-DL enables FD MCN operation in the downlink without multi-antenna UAVs, nor complex self-interference cancellation schemes.

Algorithm 1 The BUN-DL Algorithm

1: **input** Q_k, CSI for $\{R_k\rightarrow D_j\}, j\in\{1,2\}$ links
2: Each UAV R_k available for transmission chooses α_k to perform NOMA
3: **if** $R_k \in \mathcal{F}_{RD}$ **then**
4: R_k sets its timer inversely proportional to Q_k
5: **if** R_k is activated to transmit **then**
6: R_k transmits using NOMA to D_1 and D_2.
7: UAV with non-full buffer $R_i, i\neq k$ aims at receiving the BS signal, experiencing IRI.
8: **end if**
9: **else**
10: Each UAV R_i with a non-full buffer aims at receiving the shore BS signal, without IRI.
11: **end if**
12: Packets from the buffers are discarded, according to ACKs from D_1 and D_2, exploiting packet IDs
13: **output** Links $\{R_k\rightarrow D_j\}, j\in\{1,2\}$ to transmit and $R_i \in \mathcal{F}_{SR}$ to receive.

D. DISCUSSION AND SUMMARY

In terms of practical implementation, BUN-DL employs each UAV R_k with a non-empty buffer to calculate the power allocation coefficients $\alpha_{k,\min}$ and $\alpha_{k,\max}$ to examine whether NOMA communication is possible. As $\{R\rightarrow D\}$ CSI at each UAV R_k is available, the α_k values can be precisely computed. Next, $\mathcal{F}_{RD} \neq \emptyset$, $R_k \in \mathcal{F}_{RD}$ is activated to transmit, being the UAV with the maximum number of

packets. Towards avoiding UAV selection with outdated CSI, due to centralized CSI acquisition and processing, priority to distributed operation should be given [32], [33].

Meanwhile, power allocation in NOMA demands the packet decoding order at each maritime node. So, the activated transmitting UAV R_k notifies the maritime nodes on which decoding strategy they have to follow. This can be achieved by adding one bit to the packet's header. In the case of two maritime nodes, when the bit value is "0", D_1 will adopt SIC and decode its packet without interference after decoding and subtracting the D_2'a packet. At the same time, D_2 will decode its packet by considering the signal of D_1, as interference. If the bit value is "1", the reverse strategy is followed.

Finally, with regard to complexity, it must be noted that in the worst case scenario where all K UAV buffers are neither empty nor full, there will be $K \times (K-1)$ combinations, in order to perform successive shore BS and UAV transmissions. As a result, the worst case complexity to perform UAV selection in BUN-DL is $\mathcal{O}(K^2)$.

IV. UPLINK

Here, BA and UAV-aided NOMA in the uplink (BUN-UL), employing dynamic decoding ordering at each UAV to establish reliable MCN connectivity with a shore BS is presented. BUN-UL is characterized by low implementation complexity, since the maritime nodes do not need to obtain any CSI, and as a consequence, it can be very useful in MCNs with resource-constrained maritime devices.

A. {S→R} TRANSMISSION

In the uplink $\{S \rightarrow R\}$ links, BUN-UL does not assume fixed signal ordering and prompts the UAVs to consider the received CSI while determining the decoding order, increasing in this way, the probability for SIC of the signals of the N maritime nodes. In greater detail, BUN-UL leverages the buffering capabilities of the UAVs, even if SIC fails to decode all N packets, transmitted in this time-slot. Then, the UAVs store the packets that were decoded successfully, as long as the corresponding sub-buffers have available space. In such cases, BUN-UL allows UAV to store and transmit a subset of packets, and in this way, the length of each sub-buffer might be different.

When an $\{S \rightarrow R\}$ transmission takes place, NOMA is employed to concurrently transmit the symbols of the N maritime sources, i.e., $x_1, \ldots, x_N$ with $\mathbb{E}[|x_n|^2] = 1$, $n \in \{1, 2, \ldots, N\}$.

Next, UAV R_k receives signal y_k, including the information symbols of the N maritime sources, being given by

$$y_k = \sum_{n=1}^{N} h_{S_n R_k} \sqrt{P_{S_n}} x_n + \eta_{R_k}; \quad (14)$$

where η_{R_k} corresponds to AWGN at the UAV R_k.

During SIC operation, S_n's signal is successfully received by R_k if

$$\Gamma_{S_n R_k}(P_{S_n}) \triangleq \frac{|h_{S_n R_k}|^2 P_{S_n}}{\sum_{i=n+1}^{N} |h_{S_i R_k}|^2 P_{S_i} + \sigma_{R_k}^2} \geq 2^{r_{S_n}} - 1; \quad (15)$$

considering that R_k has decoded the preceding $N-n$ signals, and subtracted them from y_k prior to decoding S_n's signal.

For signal ordering, the dynamic SIC process of [34] is used, based on CSI calculated by the UAVs, i.e. measuring the instantaneous signal power at the reception. The set Φ contains all the possible decoding orders and UAV R_k decides on the permutation ϕ_k, $\phi_k \in \Phi$, being necessary to order the signals. After broadcasting, each UAV is employed to sequentially decode the signals, following the source ordering as $\phi_{k,1}, \phi_{k,2}, \ldots, \phi_{k,N}$, based on their respective channel gains $g_{\phi_{k,1} R_k} \geq g_{\phi_{k,2} R_k} \geq \cdots \geq g_{\phi_{k,N} R_k}$, as the maritime nodes adopt equal transmit power levels. Thus, initially, the signal with the highest power is decoded and the other signals are treated as interference. After, the decoded signal is subtracted and SIC moves on to the signal with second highest power. These steps continue until the signal of the source with index $\phi_{k,N}$, i.e. the one with the lowest power at the reception, is decoded without any interference. The feasible $\{S \rightarrow R\}$ link set is denoted by $\mathcal{F}_{SR}^n$ with cardinality of F_{SR}^n, considering that after SIC, the UAV has managed to decode packets from n maritime sources, and that the set's members fulfill (15).

B. {R→D} TRANSMISSION

Since in many maritime scenarios, such as mission critical services or remote control, low latency is required, BUN-UL prioritizes transmissions in the $\{R \rightarrow D\}$ links, as long as packets exist in the UAVs' buffers. Equal buffer capacity is given for each maritime source, leading to the creation of N sub-buffers, from which, the UAV relays data to the shore BS from n sources ($n \leq N$). The adoption of BUN-UL which considers BSI for UAV selection, facilitates the activated UAV to avoid sub-buffer overflow cases, thus safeguarding the MCN's diversity. Also, in the $\{R \rightarrow D\}$ link, we consider that CSI at the transmitter (CSIT) is available, being necessary for each UAV to decide the data rate that will be employed to forward the packets to the shore BS. So, even though a UAV might satisfy the BUN-UL BSI criterion, the quality of its $\{R \rightarrow D\}$ link might not be sufficient to transmit towards the shore BS.

In practical settings, each maritime source might adopt a different rate r_{S_n}, as heterogeneous services take place in the MCN. As a result, towards avoiding buffer overflow or starvation, in the MCN uplink, the activated UAV R_k will relay a combined packet to the shore BS, with the maximum rate being equal to the sum of the rates of the N maritime sources, i.e. $r_{\max} = \sum_{n=1}^{N} r_{S_n}$. Thus, if N packets are scheduled for transmission, the SNR at the shore BS must satisfy

$$\Gamma_{R_k D}(P_{R_k}) \triangleq \frac{|h_{R_k D}|^2 P_{R_k}}{\sigma_D^2} \geq 2^{r_{\max}} - 1. \quad (16)$$

On the other hand, the packet, including the data of N maritime nodes will not be forwarded to the BS, if $\gamma_{R_kD} < 2^{r_{\max}} - 1$. So, the outage probability of transmitting data of N sources by R_k is given by

$$p_{\text{out}\{R\to D\}} \triangleq \Pr\left[|h_{R_kD}|^2 < \frac{(2^{r_{\max}} - 1)\sigma_D^2}{P_{R_k}}\right]. \tag{17}$$

It should be emphasized that BUN-UL provides additional scheduling flexibility to the NOMA communication, since the amount of stored and transmitted packets might be less than N. In the worst case the wireless channel will only allow the transmission of a packet for the maritime source, demanding the minimum rate level. Here, the probability in (17) depends on $r_{\min}$, where $r_{\min} = \min\{r_1, r_2, \ldots, r_N\}$ is the rate for the service with the minimum rate requirement.

In the MCN uplink, as CSIT for transmitting in $\{R\to D\}$ links is available, the activated UAV performs an adaptive rate transmission by selecting a rate to satisfy the demands of as many maritime sources as possible. By $\mathcal{F}_{RD}^n$, the feasible $\{R\to D\}$ link set is represented with cardinality F_{RD}^n, where the respective UAVs can relay packets from n maritime sources. Then, if an $\{R\to D\}$ link can serve a packet transmission with rate r_{S_i}, $i \in \{1, 2, \ldots, N\}$ and still, the UAV has an empty buffer, that link is considered to be in outage.

C. BUN-UL ALGORITHMIC DESCRIPTION

In general, the reliability of NOMA depends on highly asymmetric user pairing, in terms of CSI, rates or both. So, in this UAV swarm-aided MCN, the presence of BA UAVs offers high degrees of freedom (DoF) to BUN-UL to avoid outages. As a consequence, UAV selection with BUN-UL exploits these DoF, employing broadcasting by the maritime sources without any power control procedures or complex user pairing, thus without necessitating CSIT in the $\{S\to R\}$ links. Instead, BUN-UL is based on BSI and CSIT at the UAVs. In greater detail, in the $\{S\to R\}$ links, dynamic user ordering only requires CSI at the reception to define $\mathcal{F}_{SR}^n$, while CSIT is used in the $\{R\to D\}$ links to determine $\mathcal{F}_{RD}^n$. Moreover, as a UAV swarm-aided MCN is assumed, power control by the maritime sources might not be practical, as increasing the probability for SIC at one UAV might degrade SIC performance at a different UAV in the swarm. So, in BUN-UL, maritime sources adopt fixed power transmissions. Algorithm 2 presents the steps of BUN-UL at an arbitrary time-slot.

D. DISCUSSION AND SUMMARY

It must be noted that BUN-UL can operate in a centralized or distributed manner. When centralized operation is adopted, the shore BS is responsible to acquire the CSI and BSI of all the UAVs and conduct UAV selection prior to transmission. On the other hand, when distributed operation is employed,

Algorithm 2 The BUN-UL Algorithm

input $\mathcal{F}_{RD}^n$, $n \in \{1, 2, \ldots, N\}$
if $\mathcal{F}_{RD}^n = \emptyset$, $\forall n$ **then**
  The N maritime sources transmit to the K UAVs in the swarm.
  $Q_j \leftarrow Q_j + r_j^\dagger$, $r_j^\dagger \in \{r_{\min}, \ldots, r_{\max}\}$ $\forall j \in \mathcal{F}_{SR}^m$, $m \in \{1, 2, \ldots, N\}$
else
  $n' = \arg\max_n \mathcal{F}_{RD}^n$
  $i' = \arg\max_{i\in\mathcal{F}_{RD}^{n'}} Q_{i,S_l}$
  if more than one UAV sub-buffers have equal maximum length **then**
    i^* is randomly selected from the set of UAVs in i'.
  else
    $i^* = i'$
  end if
  $Q_i^* \leftarrow Q_i^* - r_i^*$, $r_i^* \in \{r_{\min}, \ldots, r_{\max}\}$
end if
Output Link $\{R_{i^*} \to D\}$ is employed for transmission with rate $r^* \in \{r_{\min}, \ldots, r_{\max}\}$ towards the shore BS or the set of links in $\mathcal{F}_{SR}^n$ support the transmission of packets rate $r^\dagger \in \{r_{\min}, \ldots, r_{\max}\}$ from n source, using NOMA, where $n \le N$.

UAV selection depends on the use of distributed timers at the UAVs. In this case, the UAVs that provide links that can support the desired transmission rates and have packets in their buffers, set the timer values based on the number of packets from various maritime nodes that can be forwarded to the shore BS and the maximum sub-buffer length. Similar distributed schemes have been presented in [35] for relay selection in the uplink of multi-relay networks and in [36] in the case of downlink communications with multiple relays.

Finally, regarding complexity, in the worst case, where all the UAVs participate in the selection process, as their queues will be neither empty nor full, the CSI and BSI of K nodes must be acquired. Thus, in this case, the complexity to conduct UAV selection in BUN-UL is $\mathcal{O}(2K)$.

V. PERFORMANCE EVALUATION

Here, average sum-rate comparisons are presented, including other NOMA and OMA algorithms in downlink and uplink scenarios. Regarding the MCN topology: 1) the shore BS is located at (0, 0, 10) m, and 2) UAVs and maritime nodes are randomly located in an area with x-axis coordinates within [0, 100] m and y-axis coordinates within [−100, 100] m, being fixed throughout the simulation. Also, UAVs fly at a height of 300 m. For the wireless channel parameters, we adopt the values in [24], while heterogeneous rate requirements are assumed in each communication direction, corresponding to different QoS levels. Finally, a varying size of the UAV swarm K is considered, aiming to evaluate its

TABLE 3. Simulation parameters.

Parameter	Value
No. of UAVs in the swarm K	{2, 4, 6}
No. of transmissions per transmit power value	10^4
Buffer size L	100 bits
Transmission rate r_{USV} - downlink	2 bps/Hz
Transmission rate r_{Buoy} - downlink	1 bps/Hz
Transmission rate r_{USV} - uplink	{4, 5} bps/Hz
Transmission rate r_{Buoy} - uplink	0.5 bps/Hz
Transmit power range of each transmitter P_T	[0, 30] dBm
Noise power at each receiver σ^2	- 107 dBm
Carrier frequency f	2 GHz
Propagation constants $\alpha, b, \eta_{LoS}, \eta_{NLoS}$	5.0188, 0.3511, 0.1, 21
UAV altitude h_U	300 m

impact on the MCN's reliability. The simulation parameters are listed in Table 3.

A. DOWNLINK UAV SWARM-AIDED MCN

Starting with the downlink case, average sum-rate results for BUN-DL, buffer-aided half-duplex (BA-HD) NOMA and BA-HD OMA are presented. An MCN with a shore BS transmitting through K UAVs towards two maritime nodes (a USV and a buoy) is considered. Such a topology can correspond to an edge network where the shore BS forwards data and the results of data analytics computations towards the USV to improve its trajectory or to support a specific task, leveraging its own and the buoy's data, e.g. surveying maritime infrastructures. In this case, the downlink transmission of data and computations by the shore BS allows the maritime nodes to avoid demanding local data processing, in terms of hardware and energy requirements.

Fig. 2 depicts the average sum-rate results for the three multiple access algorithms when $K = 4$. It is evident that the FD capability of BUN-DL due to successive relaying allows it to significantly increase the average sum-rate in the MCN. Moreover, the flexible HD operation due to the buffering capabilities of the UAVs helps it to avoid outages when successive transmissions are not possible due to IRI. Then, BA-HD-NOMA surpasses its OMA equivalent due to efficient power allocation for the signals of the two maritime nodes. It must be noted that the considered MCN comprises maritime nodes that exhibit channel asymmetry due to different locations, as well as rate asymmetries, thus exploiting the potential of the adopted power allocation method for NOMA [31].

Next, Fig. 3 depicts the sum-rate performance for varying K, focusing on the BUN-DL multiple access scheme. It can be observed that, as successive relaying introduces IRI, when a higher number of UAVs is available, additional degrees of freedom in UAV selection are provided. As a result, the $K = 6$ case offers the highest sum-rate, with $K = 4$ closely following. Moreover, the performance gain reduces as K increases, as the considered rate requirements are adequately satisfied when $K = 4$. This observation highlights the limited chances to achieve successive relaying when $K = 2$, since IRI

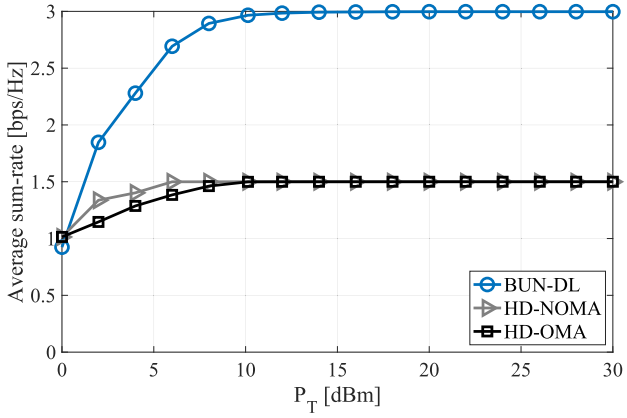

FIGURE 2. Performance comparisons, in terms of average sum-rate for different multiple access algorithms when $K = 4$, $r_{\text{USV}} = 2$ bps/Hz and $r_{\text{Buoy}} = 1$ bps/Hz.

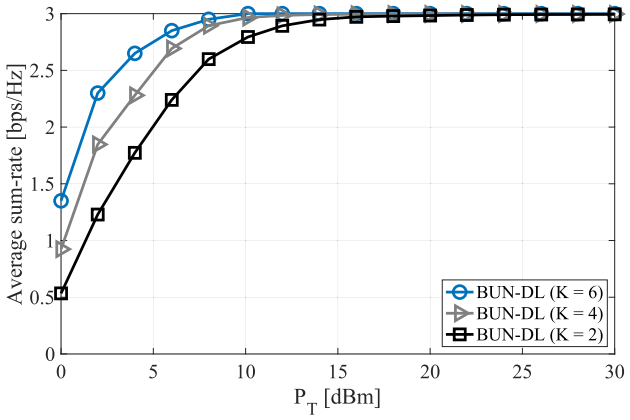

FIGURE 3. Performance comparisons, in terms of average sum-rate for BUN-DL with varying UAV swarm size K when $r_{\text{USV}} = 2$ bps/Hz and $r_{\text{Buoy}} = 1$ bps/Hz.

cannot be efficiently avoided by the small number of available UAVs in the MCN.

Then, average delay results for the three multiple access schemes with $K = 4$ UAVs in the MCN, are given in Fig. 4. Here, HD-OMA, due to fixed scheduling and the lack of interference can easily support the low service rate of the buoy, even for low SNR values. However, the high rate required by the USV cannot be easily supported and its delay performance improves only after 10 dBm. On the other hand, BUN-DL ensures that both maritime nodes can be served with reduced delay after 5 dBm and as wireless conditions improve, it outperforms HD-OMA. Moreover, BUN-DL reaches the delay performance of HD-NOMA after 10 dBm, due to its FD capabilities, exploiting the successive shore BS and UAV transmissions in the MCN. More importantly, FD operation allows BUN-DL to transmit more packets in the network, thus greatly improving the sum-rate-delay trade-off over the other two multiple access schemes.

From these comparisons, it can be observed that BUN-DL better supports MCNs for a wide gamut of transmit power

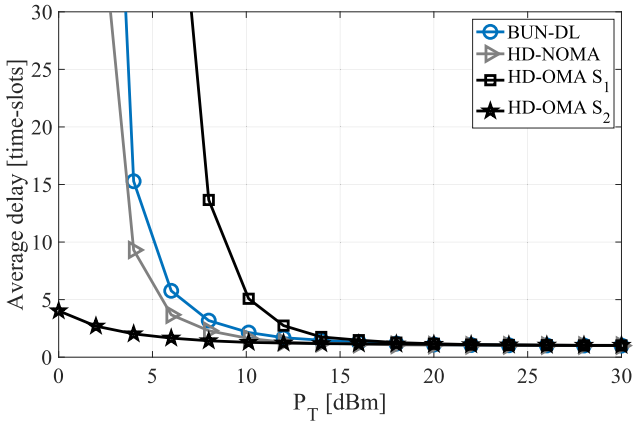

FIGURE 4. Average delay comparisons for different multiple access algorithms when $K = 4$, $r_{\text{USV}} = 2$ bps/Hz and $r_{\text{Buoy}} = 1$ bps/Hz.

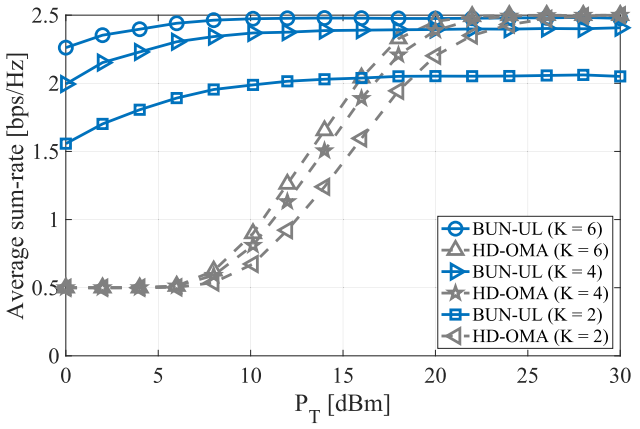

FIGURE 5. Average sum-rate comparisons for BUN-UL and HD-OMA algorithms and a varying number of UAVs when $r_{\text{USV}} = 4$ bps/Hz and $r_{\text{Buoy}} = 0.5$ bps/Hz.

levels, easily outperforming the HD multiple access schemes without requiring multi-antenna UAVs to be available in the MCN. Furthermore, if additional UAVs are employed, the MCN's reliability is significantly improved. Considering that the number of maritime services is expected to continuously increase in the context of Industry 4.0 and integrated satellite-aerial-terrestrial networks, the availability and use of UAVs in MCNs is expected to increase.

B. UPLINK UAV SWARM-AIDED MCN

In the uplink case, BUN-UL and HD-OMA sum-rate comparisons are presented. In this scenario, an MCN comprising three maritime sources is assumed, including a USV with rate requirement $r_{\text{USV}} \in \{4, 5\}$ bps/Hz and a set of two buoys, each having a rate requirement $r_{\text{Buoy}} = 0.5$ bps/Hz. Regarding the operation of the HD-OMA algorithm, it is assumed that at an arbitrary time-slot, a pre-determined maritime source is scheduled to transmit, in the $\{S \rightarrow R\}$ or in the $\{R \rightarrow D\}$ link, following the time division multiple access (TDMA) principle. To ensure fairness, the rate requirement for successful transmission by each source is considered to be three times the target service rate, as in the case of NOMA, at each time-slot, all maritime sources simultaneously transmit. This uplink scenario can correspond to an MCN where the USV patrols a maritime area, e.g. the perimeter of a port or maritime infrastructures and transmits video data (possibly with different qualities, depending on the application requirements) to a central location for data processing. Correspondingly, the buoys might support the operation of the USV by collecting data from their sensors, related to possible intrusion incidents below the water surface or they can independently collect environmental monitoring data for another maritime service.

Fig. 5 shows the average sum-rate comparison for different UAV swarm size K when $r_{\text{USV}} = 4$ bps/Hz and $r_{\text{Buoy}} = 0.5$ bps/Hz. In the case of BUN-UL, as the number of UAVs increases, the sum-rate performance significantly improves. In greater detail, when more UAVs are available in the MCN, higher probability for asymmetric channels towards the maritime sources can be seen. Thus, assuming that a rate asymmetry already exists, the dynamic SIC enables a more robust signal decoding process at the UAVs. On the other hand, OMA cannot fulfill the desired USV rate under low P_T and is characterized by reduced sum-rate until 20 dbm. For higher P_T, BUN-UL sum-rate performance reaches a ceiling, since SIC cannot offer additional performance gains while OMA leverages high SNR to satisfy all rate requirements and has improved sum-rate due to interference-free reception.

The next comparison is illustrated in Fig. 6 where a more demanding $r_{\text{USV}} = 5$ bps/Hz is assumed. In this case, the improvement by BUN-UL is evident for a much wider SNR range, even though saturation can be seen after 20 dbm. Again, a UAV swarm of greater size facilitates NOMA operation, by providing higher link diversity and channel asymmetry. In the case of OMA, higher sum-rate is provided after 28 dbm for swarm sizes $K = 2, 4$ but r_{USV} cannot be satisfied until 16 dbm. When $K = 6$, OMA exhibits identical performance with BUN-UL only at 30 dbm.

Next, Fig. 7 illustrates the average delay performance of BUN-UL and HD-OMA for $K = 4$ UAVs. It can observed that independently of the multiple access scheme, the average delay of all three maritime sources reaches one time-slot for high SNR. As BUN-UL and HD-OMA prioritize the transmission in the $\{R \rightarrow D\}$ link, when wireless conditions improve, packets tend to remain in the UAVs' buffers for only one time-slot. Moreover, BUN-UL guarantees low-delay transmissions in a wide range of SNR conditions, since at each time-slot, more than one maritime sources can be scheduled. On the contrary, HD-OMA schedules each maritime source to transmit at either the $\{S \rightarrow R\}$ or $\{R \rightarrow D\}$ link once every three time-slots. As a result, to transmit the same number of packets in the network, HD-OMA must transmit with three times the target rate of each source. Thus, a significant average delay difference can be observed, between the two buoys, enjoying low average delay and

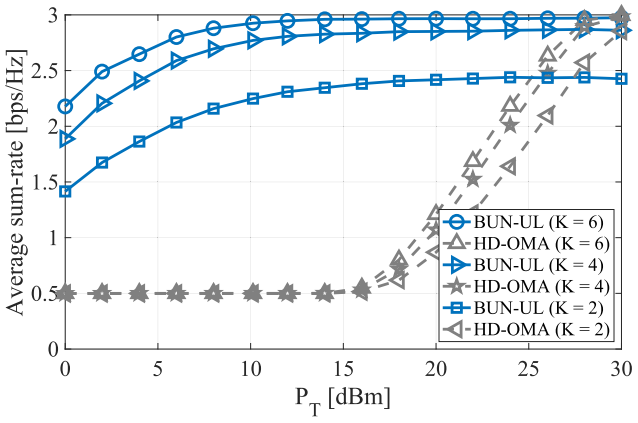

FIGURE 6. Average sum-rate comparisons for BUN-UL and HD-OMA algorithms and a varying number of UAVs when $r_{\text{USV}} = 5$ bps/Hz and $r_{\text{Buoy}} = 0.5$ bps/Hz.

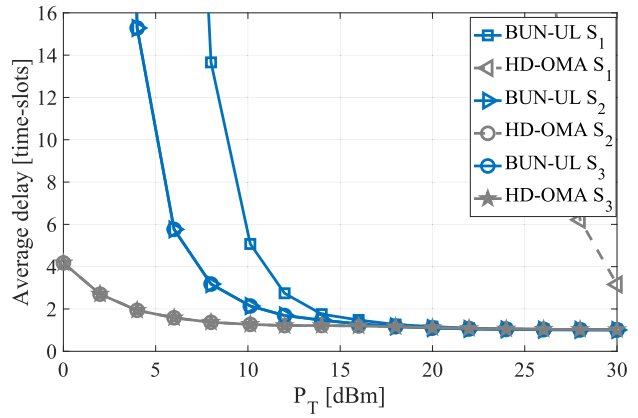

FIGURE 7. Average delay comparisons for BUN-UL and HD-OMA algorithms when $K = 4$, $r_{\text{USV}} = 4$ bps/Hz and $r_{\text{Buoy}} = 0.5$ bps/Hz.

the USV that experiences excessive delay throughout the considered SNR region.

Considering the two comparisons, it can be observed that NOMA allows the MCN to efficiently operate at lower transmit power levels by serving both high and low data rate maritime services. Still, in some cases, OMA outperforms NOMA when higher transmit power is available due to the absence of interference among the maritime nodes' signals. As a result, hybrid OMA/NOMA switching can enable the MCN to further improve its performance at the cost of slightly higher signalling overheads, needed to trigger switching between the two multiple access schemes.

VI. CONCLUSION AND FUTURE DIRECTIONS

A. CONCLUSION

In this study, a UAV swarm was considered to improve MCN connectivity. The MCN comprised maritime nodes, such as USVs, buoys and offshore platforms, desiring wireless downlink/uplink connectivity with a shore BS. In this topology, communication was established through UAVs with buffering capabilities, acting as wireless relays. In this context, downlink and uplink opportunistic UAV selection and NOMA-based algorithms were developed. In the downlink, UAVs used NOMA and allocated power to the transmitted signals, according to both rate requirements and channel state information. Then, in the uplink, dynamic decoding ordering was employed by the UAVs, improving the probability to perform successful successive interference cancellation. The proposed algorithms ensure reliable NOMA-based access to maritime nodes, improving the MCN sum-rate performance in both downlink and uplink communication.

B. FUTURE DIRECTIONS

Ongoing research mainly focuses on the fields below:

- Performance comparisons shows that approaches relying on NOMA and OMA achieve higher sum-rate under different SNR regimes. So, the design of hybrid NOMA/OMA schemes should be pursued in order to leverage the both multiple access techniques.
- Cooperation between multiple unmanned nodes may result in increased network overheads, in particular when centralized algorithms are adopted. As a result, distributed algorithms and machine learning solutions for extracting channel statistics and mobility patterns represent important research directions [37], [38], [39].
- Further areas that must be investigated are related to the integration of open and highly modular communications paradigms, such as network function virtualization (NFV) and Open Radio Access Network (O-RAN) to improve scalability in UAV swarm-aided MCNs with heterogeneous QoS requirements [40], [41].

REFERENCES

[1] I. Budhiraja, N. Kumar, S. Tyagi, and S. Tanwar, "Energy consumption minimization scheme for NOMA-based mobile edge computation networks underlaying UAV," *IEEE Syst. J.*, vol. 15, no. 4, pp. 5724–5733, Dec. 2021.

[2] N. Nomikos, E. T. Michailidis, P. Trakadas, D. Vouyioukas, H. Karl, J. Martrat, T. Zahariadis, K. Papadopoulos, and S. Voliotis, "A UAV-based moving 5G RAN for massive connectivity of mobile users and IoT devices," *Veh. Commun.*, vol. 25, Oct. 2020, Art. no. 100250.

[3] M. Vaezi, A. Azari, S. R. Khosravirad, M. Shirvanimoghaddam, M. M. Azari, D. Chasaki, and P. Popovski, "Cellular, wide-area, and non-terrestrial IoT: A survey on 5G advances and the road toward 6G," *IEEE Commun. Surveys Tuts.*, vol. 24, no. 2, pp. 1117–1174, 2nd Quart., 2022.

[4] T. Xia, M. M. Wang, J. Zhang, and L. Wang, "Maritime Internet of Things: Challenges and solutions," *IEEE Wireless Commun.*, vol. 27, no. 2, pp. 188–196, Apr. 2020.

[5] M. M. Wang, J. Zhang, and X. You, "Machine-type communication for maritime Internet of Things: A design," *IEEE Commun. Surveys Tuts.*, vol. 22, no. 4, pp. 2550–2585, 4th Quart., 2020.

[6] Y. Zeng, R. Zhang, and T. J. Lim, "Wireless communications with unmanned aerial vehicles: Opportunities and challenges," *IEEE Commun. Mag.*, vol. 54, no. 5, pp. 36–42, May 2016.

[7] Y. Wang, W. Feng, J. Wang, and T. Q. S. Quek, "Hybrid satellite-UAV-terrestrial networks for 6G ubiquitous coverage: A maritime communications perspective," *IEEE J. Sel. Areas Commun.*, vol. 39, no. 11, pp. 3475–3490, Nov. 2021.

[8] Y. Kwon, H. Baek, and J. Lim, "Uplink NOMA using power allocation for UAV-aided CSMA/CA networks," *IEEE Syst. J.*, vol. 15, no. 2, pp. 2378–2381, Jun. 2021.

[9] N. Nomikos, P. K. Gkonis, P. S. Bithas and P. Trakadas, "A survey on UAV-aided maritime communications: Deployment considerations, applications, and future challenges," *IEEE Open J. Commun. Soc.*, vol. 4, pp. 56–78, 2023
[10] S. Guan, J. Wang, C. Jiang, R. Duan, Y. Ren, and T. Q. S. Quek, "MagicNet: The maritime giant cellular network," *IEEE Commun. Mag.*, vol. 59, no. 3, pp. 117–123, Mar. 2021.
[11] F. S. Alqurashi, A. Trichili, N. Saeed, B. S. Ooi, and M.-S. Alouini, "Maritime communications: A survey on enabling technologies, opportunities, and challenges," *IEEE Internet Things J.*, vol. 10, no. 4, pp. 3525–3547, Feb. 2023.
[12] A. Giannopoulos, N. Nomikos, G. Ntroulias, T. Syriopoulos, and P. Trakadas, "Maritime federated learning for decentralized on-ship intelligence," in *Proc. Int. Conf. Artif. Intell. Appl. Innov.*, I. Maglogiannis, L. Iliadis, J. MacIntyre, and M. Dominguez, Eds. Cham: Springer Nature Switzerland, 2023, pp. 195–206.
[13] SpaceX. *Starlink Maritime*. Accessed: Apr. 2023. [Online]. Available: https://www.starlink.com/business/maritime
[14] Y. Huo, X. Dong, and S. Beatty, "Cellular communications in ocean waves for maritime Internet of Things," *IEEE Internet Things J.*, vol. 7, no. 10, pp. 9965–9979, Oct. 2020.
[15] T. Z. H. Ernest, A. S. Madhukumar, R. P. Sirigina, and A. K. Krishna, "NOMA-aided multi-UAV communications in full-duplex heterogeneous networks," *IEEE Syst. J.*, vol. 15, no. 2, pp. 2755–2766, Jun. 2021.
[16] P. S. Bithas, V. Nikolaidis, A. G. Kanatas, and G. K. Karagiannidis, "UAV-to-ground communications: Channel modeling and UAV selection," *IEEE Trans. Commun.*, vol. 68, no. 8, pp. 5135–5144, Aug. 2020.
[17] X. Li, W. Feng, J. Wang, Y. Chen, N. Ge, and C.-X. Wang, "Enabling 5G on the ocean: A hybrid satellite-UAV-terrestrial network solution," *IEEE Wireless Commun.*, vol. 27, no. 6, pp. 116–121, Dec. 2020.
[18] D. Hu, Q. Zhang, Q. Li, and J. Qin, "Joint position, decoding order, and power allocation optimization in UAV-based NOMA downlink communications," *IEEE Syst. J.*, vol. 14, no. 2, pp. 2949–2960, Jun. 2020.
[19] Z. Yao, W. Cheng, W. Zhang, T. Zhang, and H. Zhang, "The rise of UAV fleet technologies for emergency wireless communications in harsh environments," *IEEE Netw.*, vol. 36, no. 4, pp. 28–37, Jul. 2022.
[20] J. Wang, H. Zhou, Y. Li, Q. Sun, Y. Wu, S. Jin, T. Q. S. Quek, and C. Xu, "Wireless channel models for maritime communications," *IEEE Access*, vol. 6, pp. 68070–68088, 2018.
[21] M. W. Akhtar and N. Saeed, "Uavs-enabled maritime communications: Opportunities and challenges," *IEEE Syst. Man, Cybern. Mag.*, vol. 9, no. 3, pp. 2–8, 2023.
[22] H. Luo, J. Wang, F. Bu, R. Ruby, K. Wu, and Z. Guo, "Recent progress of air/water cross-boundary communications for underwater sensor networks: A review," *IEEE Sensors J.*, vol. 22, no. 9, pp. 8360–8382, May 2022.
[23] X. Fang, W. Feng, Y. Wang, Y. Chen, N. Ge, Z. Ding, and H. Zhu, "NOMA-based hybrid satellite-UAV-terrestrial networks for 6G maritime coverage," *IEEE Trans. Wireless Commun.*, vol. 22, no. 1, pp. 138–152, Jan. 2023.
[24] R. Tang, W. Feng, Y. Chen, and N. Ge, "NOMA-based UAV communications for maritime coverage enhancement," *China Commun.*, vol. 18, no. 4, pp. 230–243, Apr. 2021.
[25] R. Ma, R. Wang, G. Liu, H.-H. Chen, and Z. Qin, "UAV-assisted data collection for ocean monitoring networks," *IEEE Netw.*, vol. 34, no. 6, pp. 250–258, Nov. 2020.
[26] R. Ma, R. Wang, G. Liu, W. Meng, and X. Liu, "UAV-aided cooperative data collection scheme for ocean monitoring networks," *IEEE Internet Things J.*, vol. 8, no. 17, pp. 13222–13236, Sep. 2021.
[27] N. Nomikos, A. Giannopoulos, P. Trakadas, and G. K. Karagiannidis, "Uplink NOMA for UAV-aided maritime Internet-of-Things," in *Proc. 19th Int. Conf. Design Reliable Commun. Netw. (DRCN)*, Apr. 2023, pp. 1–6.
[28] A. A. Nasir, H. D. Tuan, T. Q. Duong, and H. V. Poor, "UAV-enabled communication using NOMA," *IEEE Trans. Commun.*, vol. 67, no. 7, pp. 5126–5138, Jul. 2019.
[29] Y. Chen, W. Feng, and G. Zheng, "Optimum placement of UAV as relays," *IEEE Commun. Lett.*, vol. 22, no. 2, pp. 248–251, Feb. 2018.
[30] Q. Zhang, Z. Liang, Q. Li, and J. Qin, "Buffer-aided non-orthogonal multiple access relaying systems in Rayleigh fading channels," *IEEE Trans. Commun.*, vol. 65, no. 1, pp. 95–106, Jan. 2017.
[31] N. Nomikos, T. Charalambous, D. Vouyioukas, G. K. Karagiannidis, and R. Wichman, "Hybrid NOMA/OMA with buffer-aided relay selection in cooperative networks," *IEEE J. Sel. Topics Signal Process.*, vol. 13, no. 3, pp. 524–537, Jun. 2019.
[32] N. Nomikos, T. Charalambous, D. Vouyioukas, and G. K. Karagiannidis, "Low-complexity buffer-aided link selection with outdated CSI and feedback errors," *IEEE Trans. Commun.*, vol. 66, no. 8, pp. 3694–3706, Aug. 2018.
[33] N. Nomikos, D. Poulimeneas, T. Charalambous, I. Krikidis, D. Vouyioukas, and M. Johansson, "Delay- and diversity-aware buffer-aided relay selection policies in cooperative networks," *IEEE Access*, vol. 6, pp. 73531–73547, 2018.
[34] J. Wang, B. Xia, K. Xiao, Y. Gao, and S. Ma, "Outage performance analysis for wireless non-orthogonal multiple access systems," *IEEE Access*, vol. 6, pp. 3611–3618, 2018.
[35] N. Nomikos, E. T. Michailidis, P. Trakadas, D. Vouyioukas, T. Zahariadis, and I. Krikidis, "Flex-NOMA: Exploiting buffer-aided relay selection for massive connectivity in the 5G uplink," *IEEE Access*, vol. 7, pp. 88743–88755, 2019.
[36] A. Bletsas, A. Khisti, D. P. Reed, and A. Lippman, "A simple cooperative diversity method based on network path selection," *IEEE J. Sel. Areas Commun.*, vol. 24, no. 3, pp. 659–672, Mar. 2006.
[37] N. Nomikos, M. S. Talebi, T. Charalambous, and R. Wichman, "Bandit-based power control in full-duplex cooperative relay networks with strict-sense stationary and non-stationary wireless communication channels," *IEEE Open J. Commun. Soc.*, vol. 3, pp. 366–378, 2022.
[38] A. Giannopoulos, S. Spantideas, N. Nomikos, A. Kalafatelis, and P. Trakadas, "Learning to fulfill the user demands in 5G-enabled wireless networks through power allocation: A reinforcement learning approach," in *Proc. 19th Int. Conf. Design Reliable Commun. Netw. (DRCN)*, Apr. 2023, pp. 1–7.
[39] J.-M. Kang, I.-M. Kim, and C.-J. Chun, "Deep learning-based MIMO-NOMA with imperfect SIC decoding," *IEEE Syst. J.*, vol. 14, no. 3, pp. 3414–3417, Sep. 2020.
[40] W. Bekri, R. Jmal, and L. C. Fourati, "Softwarized Internet of Things network monitoring," *IEEE Syst. J.*, vol. 15, no. 1, pp. 826–834, Mar. 2021.
[41] A. Giannopoulos, S. Spantideas, N. Kapsalis, P. Gkonis, L. Sarakis, C. Capsalis, M. Vecchio, and P. Trakadas, "Supporting intelligence in disaggregated open radio access networks: Architectural principles, AI/ML workflow, and use cases," *IEEE Access*, vol. 10, pp. 39580–39595, 2022.

NIKOLAOS NOMIKOS (Senior Member, IEEE) received the Diploma degree in electrical engineering and computer technology from the University of Patras, Greece, in 2009, and the M.Sc. and Ph.D. degrees from the Information and Communication Systems Engineering Department, University of the Aegean, Samos, Greece, in 2011 and 2014, respectively. He is currently a Senior Researcher with the Department of Ports Management and Shipping, National and Kapodistrian University of Athens. His research interests include 6G communications, NOMA, and machine learning-aided wireless networks. He is a member of the IEEE Communications Society and the Technical Chamber of Greece. He is an Associate Editor of *Frontiers in Communications and Networks*.

ANASTASIOS GIANNOPOULOS (Member, IEEE) received the Dipl.-Ing. degree in electrical and computer engineering and the Ph.D. degree from the National Technical University of Athens (NTUA). He is currently an Electrical and Computer Engineering Researcher with the Department of Ports Management and Shipping, National and Kapodistrian University of Athens. He has more than 35 scientific publications. His research interests include wireless network optimization, machine learning, maritime communications, and multi-dimensional analysis.

ALEXANDROS KALAFATELIS (Graduate Student Member, IEEE) received the B.Sc. (Hons.) degree in biomedical sciences from the University of East London and the B.Eng. degree in electrical engineering and the M.Sc. degree in intelligent management of renewable energy systems from the National and Kapodistrian University of Athens (NKUA), where he is currently pursuing the Ph.D. degree with the Department of Ports Management and Shipping. Since 2021, he has been a Research Scientist and an Engineer with FOUR DOT INFINITY. Part of his research has been conducted in the framework of several European-funded research and development projects. His current research interests include predictive maintenance applications utilizing federated learning, focusing on the development of secure aggregations tailored for the maritime industry.

VOLKAN ÖZDURAN (Member, IEEE) graduated from the Department of Electronics, Soke Technical High School, Aydin, Turkey, in 1997, and the A.Sc. degree (Hons.) in industrial electronics and the B.Sc., M.Sc., and Ph.D. degrees in electrical and electronics engineering from Istanbul University, Istanbul, Turkey, in 2002, 2005, 2008, and 2015, respectively. During the Ph.D. studies, he was with the Department of Electrical Engineering, Dynamic Spectrum Management (DSM) Research Group, Stanford University, Stanford, CA, USA, the Department of Electrical Engineering, California Institute of Technology (CALTECH), Pasadena, CA, USA, and the Department of Electrical Engineering, Princeton University, Princeton, NJ, USA. He received the Docent title from the Turkish Interuniversity Council, Ankara, Turkey, in 2022. His current research interests include various aspects of the 6G wireless networks.

PANAGIOTIS TRAKADAS received the Dipl.-Ing. degree in electrical and computer engineering and the Ph.D. degree from the National Technical University of Athens (NTUA). In the past, he was with the Hellenic Aerospace Industry (HAI), as a Senior Engineer, on the design of military wireless telecommunications systems, and the Hellenic Authority for Communications Security and Privacy, where he held the position of the Director of the Division for the Assurance of Infrastructures and Telecommunications Services Privacy. He is currently an Associate Professor with the National and Kapodistrian University of Athens. He has been actively involved in many EU FP7 and H2020 research projects. He has published more than 130 papers in magazines, journals, and conference proceedings. His research interests include wireless and mobile communications, wireless sensor networking, network function virtualization, and cloud computing. He is a Reviewer of several journals, including IEEE Transactions on Communications and IEEE Transactions on Electromagnetic Compatibility journals.

GEORGE K. KARAGIANNIDIS (Fellow, IEEE) is currently a Professor with the Department of Electrical and Computer Engineering, Aristotle University of Thessaloniki, Greece. He is also a Faculty Fellow with the Cyber Security Systems and Applied AI Research Center, Lebanese American University. His research interests include wireless communications systems and networks, signal processing, optical wireless communications, and wireless power transfer and applications. He has received three prestigious awards, such as the 2022 Humboldt Research Award from Alexander von Humboldt Foundation, the 2021 IEEE ComSoc RCC Technical Recognition Award, and the 2018 IEEE ComSoc SPCE Technical Recognition Award. He is one of the highly-cited authors across all areas of electrical engineering, recognized by Clarivate Analytics as Web-of-Science a Highly-Cited Researcher for eight consecutive years, from 2015 to 2022. He was a past editor in several IEEE journals and from 2012 to 2015, he was the Editor-in-Chief of IEEE Communications Letters. From September 2018 to June 2022, he served as an Associate Editor-in-Chief for IEEE Open Journal of Communications Society.